Electromagnetic Performance Analysis of Novel Multi-band Metamaterial FSS for Millimeter Wave Radome Applications

Shiv Narayan[1], **Shamala Joshi B.**[1], **Raveendranath U. Nair**[1] **and R M Jha**[1]

Abstract: The electromagnetic design and performance analysis of dual/ multi-band metamaterial frequency selective surface (FSS) structures have been carried out for radome applications in microwave and millimeter wave frequency regimes. The proposed metamaterial FSS structure, consisting of cascaded MNG (mu-negative) and DPS (double positive) layers, exhibits dual-band transmission responses at V-band and W-band. Excellent transmission efficiency (more than 95%) has been obtained over the frequency range 45.8-53.1 GHz at first resonance, and from 93.0-97.1 GHz at second resonance. The incorporation of additional DPS layer to the proposed metamaterial-FSS structure facilitates multiband bandpass characteristics at 30 GHz (in Ka-band), 64 GHz (in V-band), and 93.6 GHz (in W-band). The reflection and insertion phase delay characteristics are also analyzed at high incidence angles in view of streamlined airborne nosecone radome applications.

Keywords: Metamaterial, FSS, Dual-band metamaterial-FSS, Transmission line transfer matrix method, MMW

1 Introduction

The devices and components operating in the *millimeter wave* (MMW) region have the potential of revolutionizing applications in the fields of wireless communication systems, aerospace engineering, security systems etc. During the last four decades, *frequency selective surfaces* (FSS) have been widely used in the design of spatial filters, absorbers, radomes, and reflector antennas in the microwave and MMW regions. The increasing demand of multifunctional antennas for communications systems has required dual/ multi-band FSS. The dual-reflector antenna system employed in space missions such as Voyager, Galileo, Cassini, etc. with FSS based sub-reflector has made it possible to share the main reflector between different frequency bands, as reported by Samii and Tulinsteff (1993), and Wu

---

[1] CSIR-National Aerospace Laboratories, Bangalore, 560017, India

(1994). Furthermore, the modern tracking radar systems require high performance multi-band radomes, which can be realized with the incorporation of FSS structure.

The various metallic FSS structures have been widely used for dual/ multi-band applications in reflector antennas, radomes etc. Wu and Lee (1994) proposed a multi-band frequency selective surface based on concentric circular rings elements. Romeu and Samii (2000) successfully investigated FSS screen with fractal elements for dual-band operation, where the design structure was very complex and difficult to analyze. Using periodic cell perturbations, Guo *et al*. (2008) developed a dual-band FSS. Araujo *et al*. (2009) obtained dual-resonant behavior at X-band by stacking two FSS layers. However, the conventional metallic FSS cannot be used for MMW applications due to inherently high metal losses and thickness limitations of the metallic parts of the FSS unit cell. The multilayered dielectric FSS structures were also proposed by Antonopoulos *et al*. (1997), and Li and Shanjia (2000) for above mentioned applications. The EM performance of such structures however are severely degraded due to insertion loss, which is proportional to the transmission roll-off rate resulting from high energy absorption in the inter-layer dielectric spacer material.

Recently, metamaterials have attracted much interest due to their unusual electromagnetic (EM) properties, such as negative refraction leading to backward wave propagation. In the presence of EM field, the response of the system is determined by the macroscopic parameters such as permittivity and permeability of the material. By using these parameters, one can classify the medium into four categories, (Engheta and Ziolkowski (2006)) *viz. double positive* (DPS), *epsilon-negative* (ENG), *mu-negative* (MNG), and *double-negative* (DNG) medium. Artificial materials can also be realized by using DPS, ENG, and MNG properties. In view of this, the promising applications based on *metamaterial-frequency selective surfaces* (MTM-FSS) have been presented by Oraizi and Afsahi (2009), in MMW as well in optical frequency regions.

In open domain, several numerical and analytical methods have been reported for the analysis of multilayered metamaterial structures such as *Transfer Matrix Method*, (Pendry and Mackinnon (1992)), *Iterative Method,* (Cory and Zach (2004)), and *Propagation Matrix Method,* (Kong (2002)). In the present paper, the EM performance analysis of novel multilayered metamaterial FSS structures providing dual/ multi-band responses at microwave and millimeter wave frequencies has been carried out using *transmission line transfer matrix* (TLTM) method. The proposed metamaterial-FSS structure exhibits dual-band characteristics at 50 GHz and 95 GHz with superior transmission efficiency.

2 Theoretical Considerations

The EM analysis of dual/ multi-band metamaterial-FSS has been carried out by transmission line transfer matrix (TLTM) method in this work. The TLTM method is the combination of *transmission line method* (TLM) and *transfer matrix method* (TMM). According to TLM method, a multilayered metamaterial structure is represented as multiple sections of transmission line. Each section is described by characteristic impedance and propagation constant. The transfer matrix is then obtained by cascading the wave amplitude matrix and discontinuity matrix between two consecutive layers. Finally, the outgoing wave from the structure is computed from the incident wave using the transfer matrix. In TLTM method, the reflection coefficient at the surface of each layer is obtained by starting the calculation from the previous layer using the impedance matching concept. This method depends on the incidence angle, frequency, and polarization of the incidence wave and is equally applicable to both the TE and TM incident wave polarizations. The reflection and transmission coefficient of a multilayered metamaterial structure can be computed using TLTM method for different polarizations.

The side view of a dual-band metamaterial-FSS is shown in Figure 1, which consists of four layers, where two DPS layers are sandwiched between two MNG layers of same thickness. For DPS layers, the dielectric materials having high dielectric constant are considered.

The propagation constant, γ_{lz} of section l of the transmission line, which is identical for both TE and TM polarizations, can be expressed as (Oraizi and Afsahi (2007))

$$\gamma_{lz} = j\omega\sqrt{\mu_l \varepsilon_l}\cos\theta_l \tag{1}$$

where, μ_l and ε_l are the permeability and the permittivity of the lth layer, respectively.

ω is the angualar frequency. θ_l represents the incidence angle at the lth layer.

By using the Snell's law for l^{th} and $(l+1)^{th}$ layers, the angle of incidence at each layer can be computed by

$$\gamma_l \sin\theta_l = \gamma_{(l+1)}\sin\theta_{(l+1)} \tag{2}$$

The transfer matrix of a layer is expressed as

$$[T]_{(l+1)l} = [L]_{(l+1)}[I]_{(l+1)l}, \quad l = 0, 1, \dots (N-1) \tag{3}$$

where N is the number of layers. The wave amplitude matrix $[L]_{(l+1)}$ and discontinuity transfer matrix $[I]_{(l+1)l}$ can be calculated using the expressions obtained by Oraizi and Afsahi (2007).
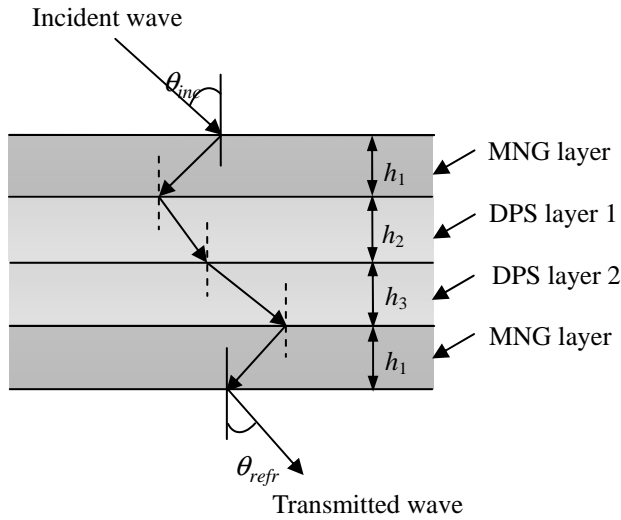
Figure 1: Side view of dual-band metamaterial-FSS structure

The transmission and reflection coefficients of the structure can be expressed by the matrix equation

$$\begin{bmatrix} t \\ 0 \end{bmatrix} = [T]_{(N+1)0} \begin{bmatrix} 1 \\ r \end{bmatrix} \tag{4}$$

where

$$[T]_{(N+1)0} = [T]_{(N+1)N} [T]_{N(N-1)} \,..... [T]_{(l+1)l} \,.... [T]_{10} \tag{5}$$

The power reflection R, and the power transmission T, of the structure can be determined as

$$R = rr^* \tag{6}$$

$$T = tt^* \tag{7}$$

According to the Lorentz and Resonance models, the permeability at the microwave frequencies may be realized by a periodic array of resonators. The complex relative permeability of the layer is computed by Pendry *et al.* (1999)

$$\mu_r = 1 - \frac{\left(f_{mp}^2 - f_{m0}^2\right)}{f^2 - f_{m0} - j\Gamma_m f} \tag{8}$$

where f_{m0} and f_{mp} are the magnetic resonant frequency and magnetic plasma frequency, respectively. The magnetic damping factor $\Gamma_m = 2pR/a\mu_0$, where R represents the metal resistance per unit volume. The magnetic resonance frequency can be expressed as

$$\omega_{m0} = c\sqrt{\frac{3p}{\pi \ln\left(\frac{2w}{d}\right) a^3}} \tag{9}$$

where p is the periodicity, w is the width of the rings, a is the radius of the ring, and d is the spacing between the rings. c denotes the speed of light. The magnetic plasma frequency of the SRR is given as

$$\omega_{mp} = \frac{\omega_{m0}}{\sqrt{1-F}} \tag{10}$$

where $F = \pi \left(a/p\right)^2$ is the fractional volume occupied by the unit cell.

The *insertion phase delay* (IPD) is defined as the delay that occurs for an electromagnetic wave *w.r.t.* the free-space transmission, when it passes through the radome wall. The IPD can be expressed, (Kozakoff (1997)) as

$$IPD = -\left(\angle T_1 + \angle T_2 + \angle T_3 + ... \angle T_n\right) - 2\pi \sum_{i=1}^{n} \frac{d_i}{\lambda_i} \cos\theta_i \tag{11}$$

where d_i and λ_i are the thickness and the wavelength of propagating wave in each layer, respectively. θ_i is the angle of incidence at each layer.

3 EM Design Aspects of Dual-band Metamaterial FSS

The proposed metamaterial-FSS structure consists of four layers as shown in Figure 2, where two DPS layers of different dielectric materials are sandwiched between the two identical MNG layers. In this design, the MNG layer consists of circular *split ring resonators* (SRR) with relative permittivity $\varepsilon_r = 1$, whereas its relative permeability is determined by equation (8). The complex relative permeability versus frequency for different separations between the rings of the SRR is shown in Figure 3.

The optimized design dimensions of SRR are periodicity, p = 1.5 mm, radius of inner ring, a = 0.5 mm, separation between the rings, d = 0.08 mm, and thickness of the ring, w = 0.12 mm. The thickness of each MNG layer is optimized to be 0.4 mm. The dielectric materials of two DPS layers are: Arlon (relative permittivity,ε_r = 4.5, electric loss tangent, $\tan\delta_e$ = 0.0026) and Rogers Ro 350 (ε_r = 3.66, $\tan\delta_e$ =
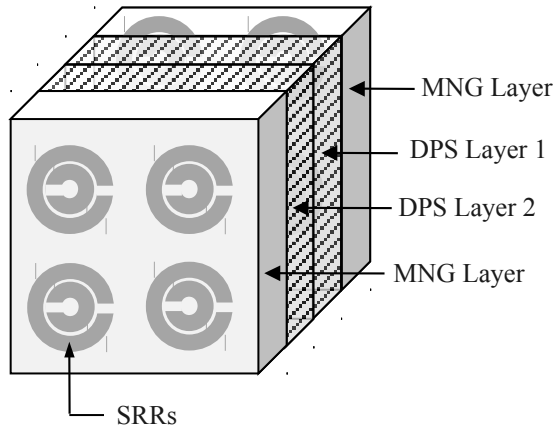
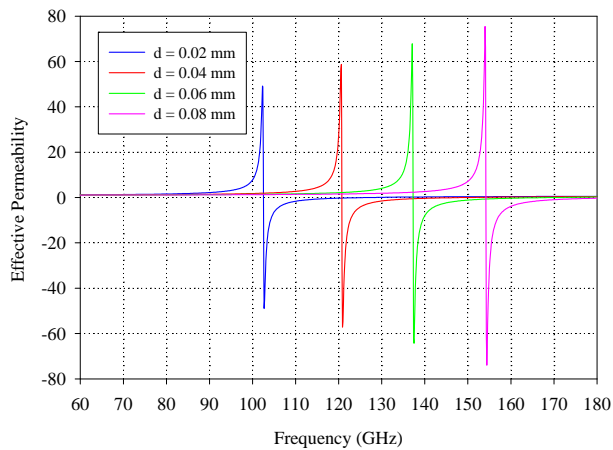Figure 2: Schematic of dual-band metamaterial FSS structure

Figure 3: Effective permeability *vs*. frequency of SRR for different separations between the rings of the SRR

0.004). The thickness of each DPS layer is optimized to be 0.8 mm. A dual-band characteristic is obtained with the optimization of the thickness of the MNG and DPS layers. The magnetic resonance frequency and magnetic plasma frequency are computed by equations (9) and (10), respectively. The insertion phase delay of the proposed metamaterial structure is then determined by equation (11).

4 EM Performance Analysis

In the present work, the EM performance of a dual/ multi-band metamaterial FSS has been investigated for TE and TM polarizations using the TLTM method. The transmission and reflection characteristics of the dual-band metamaterial-FSS structure are obtained at various angles of incidence such as 0°, 30°, 60°, and 80° for TE polarization, which are shown in Figures 4 and 5, respectively. It is observed that the proposed metamaterial-FSS structure essentially exhibits a dual-band characteristic at the frequencies 50 GHz and 95 GHz that is less sensitive to the angles of incidence.
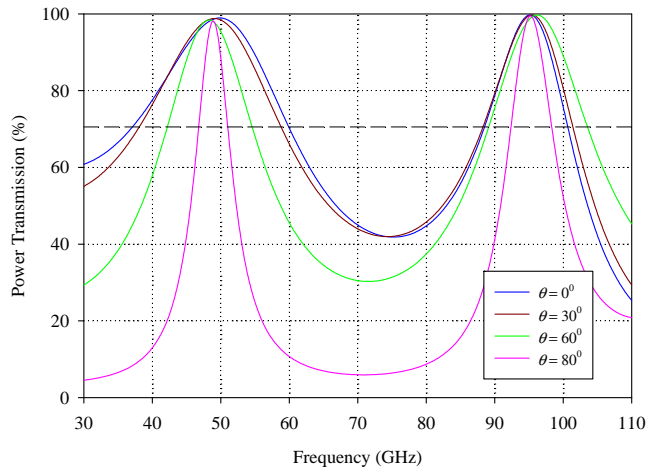

Figure 4: Power transmission characteristics of dual-band metamaterial-FSS for TE polarization at different incidence angles

The corresponding transmission and reflection characteristics are also obtained for TM polarization as shown in Figures 6 and 7, respectively. Further, the insertion phase delay characteristics of the proposed metamaterial-FSS are computed for both TE and TM polarizations at various incidence angles, as shown in Figures 8 and 9, respectively. It is observed that the IPD of the proposed metamaterial-FSS
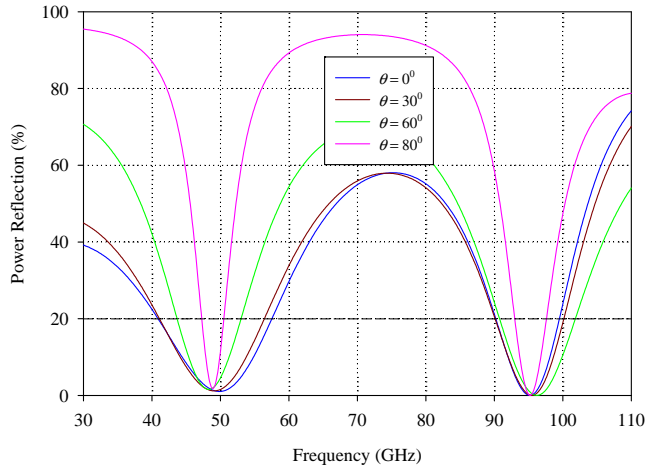
Figure 5: Power reflection characteristics of dual-band metamaterial-FSS for TE polarization at different incidence angles
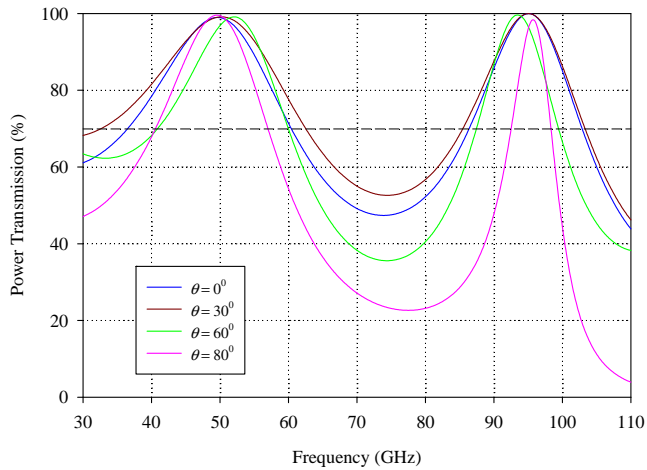
Figure 6: Power transmission characteristics of dual-band metamaterial-FSS for TM polarization at different incidence angles

does not show rapid variation *w.r.t*. the operating frequency, which is desirable for radome applications.
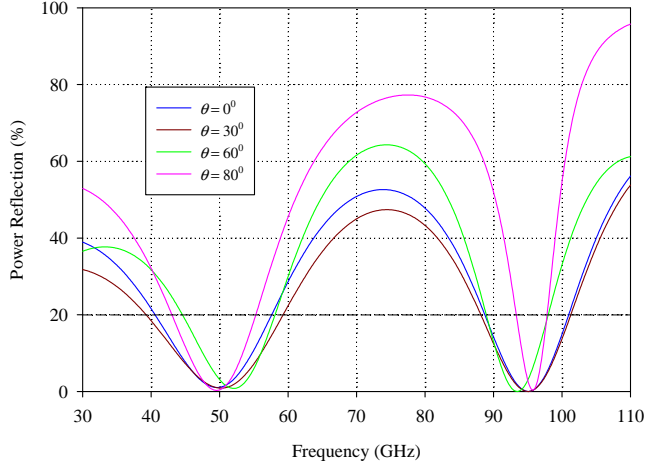

Figure 7: Power reflection characteristics of dual-band metamaterial-FSS for TM polarization at different incidence angles

Finally, the transmission and the reflection properties are analyzed at different angles of incidence for TE polarization by considering the dielectric loss of the DPS layers (Figures 10 and 11). It is observed that the transmission efficiency of the proposed structure is slightly varied as compared to the transmission response without dielectric loss (Fig. 4). The transmission efficiency is found to be reduced by 2% at first resonance, while it is reduced by 4% at second resonance.

In order to achieve multi-band characteristics, an additional DPS layer is incorporated between the Roger DPS layer and MNG layer of the proposed dual-band metamaterial-FSS structure. Thus the proposed structure becomes a five layered metamaterial-FSS structure. The dielectric material of additional DPS layer is considered to be Bakelite ($\varepsilon_r = 4.8$, tan $\delta_e = 0.002$). The optimized design parameters of the five layered metamaterial-FSS structure for multi-band operation are given in Table 1.

Further, the transmission and reflection characteristics are studied as a function of the incidence angle for TE polarization (Figures 12 and 13). It is observed that the modified metamaterial-FSS structure exhibits distinct triple band characteristics at frequencies 30 GHz, 64 GHz, and 93.6 GHz with very good transmission efficiency. In view of possible applications such as streamlined multi-band radome, the insertion phase delay is also investigated at different incidence angles (0°, 30°, 60°, and
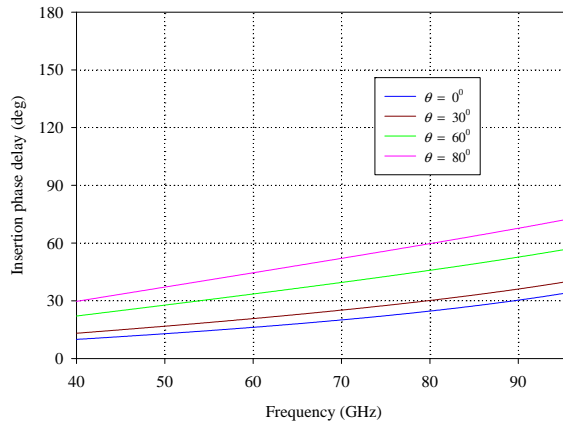
Figure 8: Insertion phase delay (IPD) of dual-band metamaterial-FSS at different incidence angles for TE polarization
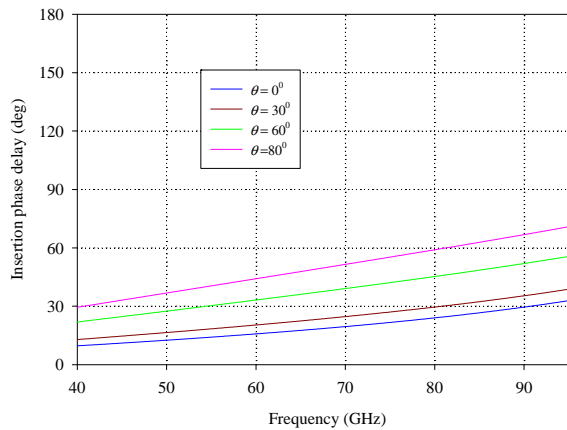

Figure 9: Insertion phase delay (IPD) of dual-band metamaterial-FSS at different incidence angles for TM polarization
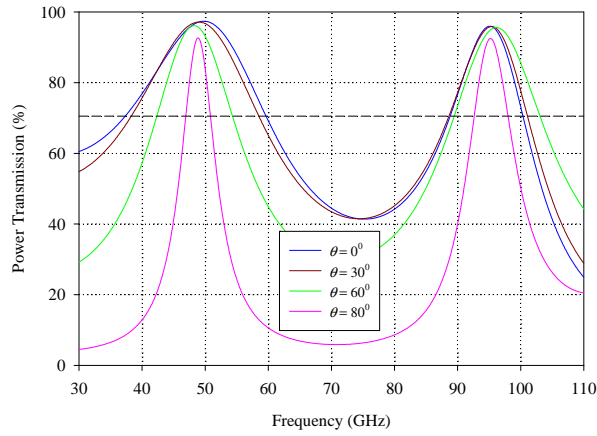
Figure 10: Power transmission characteristics of dual-band metamaterial-FSS for TE polarization at different incidence angles with **dielectric loss** of DPS layers
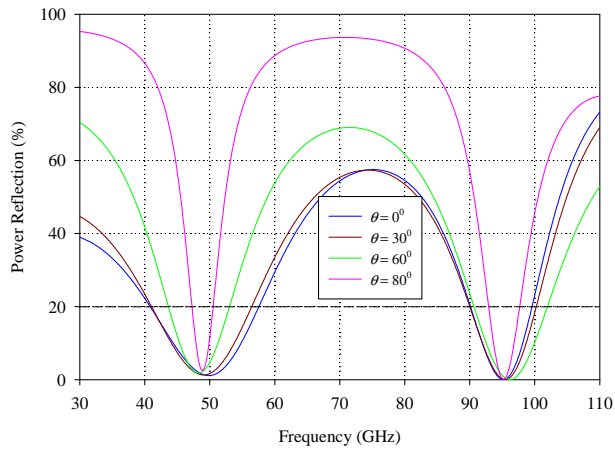

Figure 11: Power reflection characteristics of dual-band metamaterial-FSS for TE polarization at different incidence angles with **dielectric loss** of DPS layers
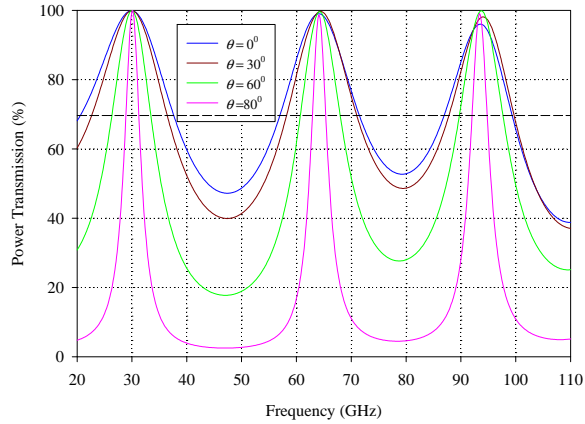
Figure 12: Power transmission characteristics of multi-band metamaterial-FSS for TE polarization at different incidence angles
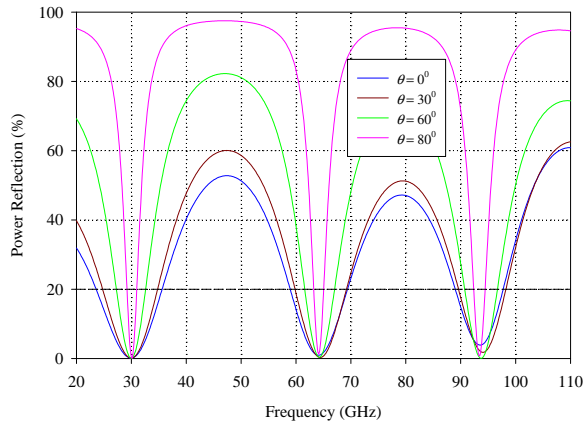

Figure 13: Power reflection characteristics of multi-band metamaterial-FSS for TE polarization at different incidence angles

Table 1: Designed parameters of metamaterial-FSS structure for multi-band operation

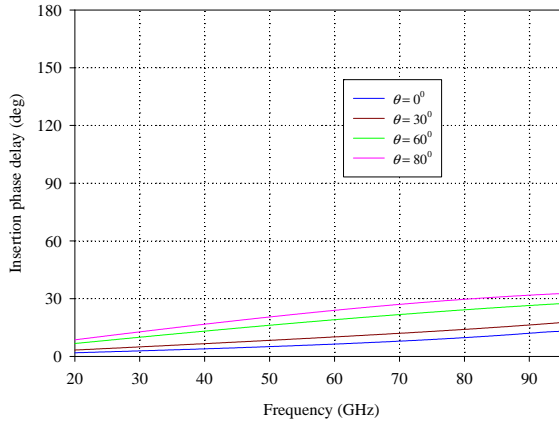| S. No.	Layers	Thickness (mm)	Dielectric constant
1.	MNG Layer	0.15	1
2.	DPS Layer 1	0.75	4.5
3.	DPS Layer 2	0.8	3.6
4.	DPS Layer 3	0.8	4.8
5.	MNG Layer	0.15	1

Figure 14: Insertion phase delay (IPD) of multi-band metamaterial-FSS at different incidence angles for TE polarization

$80°$) for TE polarization as shown in Figure 14. It is revealed that the IPD of the five layered metamaterial-FSS does not show rapid variation *w.r.t.* the operating frequency (Fig. 14), which is desirable for radome applications.

5 Conclusions

In the present work, the EM performance analysis of dual/ multi-band metamaterial-FSS structures has been investigated based on TLTM method for microwave and MMW radome applications. The proposed four-layer metamaterial-FSS structure exhibits dual-band responses at 50 GHz and 95 GHz. It shows superior transmission efficiency (more than 95%) over the frequency range 45.8-53.1 GHz at first resonance and from 93.0-97.1 GHz at second resonance. Further, the multi-band operation is also analyzed for a five-layered metamaterial-FSS structure. The superior EM performance characteristics of the metamaterial-FSS structures make

it a desirable choice for the design of both the normal incidence and the highly streamlined *nosecone* radomes. Since modern tracking radar systems require high performance multi-band radomes, these metamaterial-FSS structures are eminently suitable for such radome applications.

References

Araujo, L.M.; Manicoba, R.H.C.; Campos, A.L.P.S.; d'Assuncao, A.G. (2009): A simple dual-band frequency selective surface. *Microwave and Optical Technology Letters*, vol. 51, pp. 942-944.

Antonopoulos, C.; Cahill, R.; Parker, E.A.; Sturland, I.M. (1997): Multilayer frequency selective surfaces for millimeter and submillimeter wave applications. *Proc. IEE Microwave, Antennas and Propagation*, vol. 144, pp. 415-420.

Cory, H.; Zach, C. (2004): Wave propagation in metamaterial multilayered structures. *Microwave and Optical Technology Letters*, vol. 40, pp. 460-465.

Engheta, N.; Ziolkowski, R.W. (2006): *Metamaterials, Physics and Engineering Explorations.* Wiley, NY, ISBN 10: 0-471-76102-8.

Guo, C.; Sun, H.; Lu, X. (2008): A novel dual-band frequency selective surface with periodic cell perturbation. *Progress In Electromagnetics Research B,* vol. 9, pp. 137-149.

Kong, J.A. (2002): Electromagnetic wave interaction with stratified negative isotropic media. *Progress In Electromagnetics Research, PIER* 35, pp. 1-52.

Kozakoff, D.J. (1997): *Analysis of Radome-Enclosed Antennas*. Artech House, Boston, ISBN: 0-89006-716-3.

Li, Y.; Shanjia, X. (2000): Systematical analysis of dielectric frequency selective surface for millimeter wave applications. 2nd *International Conference on Microwave and Millimeter Wave Technology Proceedings*, Beijing, China, pp. 502-505.

Oraizi, H.; Afsahi, M. (2007): Analysis of planar dielectric multilayer as FSS by transmission line transfer matrix method (TLTMM). *Progress In Electromagnetics Research, PIER* 74, pp. 217-240.

Oraizi, H.; Afsahi, M. (2009): Design of metamaterial multilayer structure as frequency selective surfaces. *Progress In Electromagnetics Research C*, vol. 6, pp. 115-126.

Pendry, J.B.; Mackinnon, A. (1992): Calculation of photon dispersion relations.

Physical Review Letters, vol. 69, pp. 2772-2775.

Pendry, J.B.; Holden, A.J.; Robbins, D.J.; Stewart, W.J. (1999): Magnetism from conductors, and enhanced non-linear phenomena. *IEEE Transactions on Microwave Theory and Techniques*, vol. 47, pp. 2075-2084.

Romeu, J.; Samii, Y.R. (2000): Fractal FSS: A novel dual-band frequency selective surface. *IEEE Transactions on Antennas and Propagation*, vol. 48, pp. 1097-1105.

Samii, Y.R.; Tulinsteff, A.N. (1993): Diffraction analysis of frequency selective surfaces reflector antennas. *IEEE Transactions on Antennas and Propagation*, vol. 41, pp. 476-487.

Wu, T.K. (1994): Cassini frequency selective surface development. *Journal of Electromagnetics Waves and Applications,* vol. 8, pp. 1547-1561.

Wu, T.K.; Lee, S.W. (1994): Multiband frequency selective surface with multiring patch elements, *IEEE Transactions on Antennas and Propagation,* vol. 42, pp. 1484-1490.